International Journal of Biochemistry and Cell Biology 155 (2023) 106360

Contents lists available at ScienceDirect

International Journal of Biochemistry and Cell Biology

journal homepage: www.elsevier.com/locate/biocel

Epibrassinolide impaired colon tumor progression and induced autophagy in SCID mouse xenograft model via acting on cell cycle progression without affecting endoplasmic reticulum stress observed in vitro

Pinar Obakan Yerlikaya [a,b,*], Kaan Adacan [c], Ayse Karatug Kacar [d], Ajda Coker Gurkan [e], Elif Damla Arisan [f]

[a] Istanbul Medeniyet University, Faculty of Engineering and Natural Sciences, Department of Molecular Biology and Genetics, Uskudar, 34700 Istanbul, Türkiye
[b] Istanbul Medeniyet University, Science and Advanced Technology Research Center (BILTAM), Uskudar, 34700 Istanbul, Türkiye
[c] İstinye University, Molecular Cancer Research Center (ISUMKAM), Zeytinburnu, 34010 Istanbul, Türkiye
[d] Istanbul University, Faculty of Science, Department of Biology, Vezneciler, 34134 Istanbul, Türkiye
[e] Marmara University, Faculty of Arts And Sciences, Department Of Biology, Kadikoy, 34722, Istanbul, Türkiye
[f] Gebze Technical University, Institute of Biotechnology, 41400 Gebze, Kocaeli, Türkiye

ARTICLE INFO

Keywords:
Epibrassinolide
Colon cancer
SCID mouse
Autophagy
Apoptosis
Cell cycle

ABSTRACT

Epibrassinolide is a member of brassinosteroids with a polyhydroxysteroid structure similar to steroid hormones of vertebrates. It was shown that EBR decreased cell proliferation and induced apoptosis in different colon cancer cell lines without exerting a cytotoxic effect in epithelial fetal human colon cells. This finding highlighted the potential of epibrassinolide in clinical therapeutic setup. In our previous studies, we showed that epibrassinolide was able to induce apoptosis via endoplasmic reticulum stress. Recently, we also showed that endoplasmic reticulum and apoptotic stresses can be prevented via autophagic induction in non-cancerous epithelial or aggressive forms of cancer cells. Therefore, here in this study, we evaluated the anti-tumoral effect of epibrassinolide as well as the autophagy involvement in the aggressive forms of colon cancer cell lines as well as in vivo SCID mouse xenograft colon cancer model for the first time. For this purpose, SCID mouse model was used for subcutaneous injection of colon cancer cells in matrigel formulation. We found that autophagy is induced in both in vitro and in vivo models. Following tumor formation, SCID mice were treated daily with increasing concentrations of epibrassinolide for two weeks. Our findings showed that EBR inhibited the volume and diameter of the tumor in a dose-dependent manner by causing cell cycle arrest. Therefore our data suggest that epibrassinolide exerts a cytostatic effect on the agrressive form of colon cancer model in vivo, without affecting endoplasmic reticulum stress and the induction of autophagy might have role in this effect of epibrassinolide.

1. Introduction

Colon cancer is one of the common types of malignant neoplasms and shows increasing tendency in terms of both morbidity and mortality (Siegel et al., 2022, 2021). The lack of physical activity, a low-fiber and high-fat diet, obesity, tobacco use, and genetic factors are among the risk factors. Patients with metastatic colon cancer are usually treated with first- or second-line chemotherapy including oxaliplatin, 5-fluorouracil, leucovorin, irinotecan, cetuximab, and bevacizumab (Buchler et al., 2014). However, the prognosis has never been satisfying, especially for patients with metastatic lesions, and the search for better options still continue.

Brassinosteroids (BR) are polyhydroxylated phytohormones with similar structures to animal steroids. Their molecular actions can be determined during plant cell elongation, cell division, cell differentiation, and immunity. Their signaling mechanism fire by the binding of the BR ligand to the heteroligomerized receptors (BRI1 and BAK1) localized on the plant cell membrane. Upon binding of the ligand and the activation of the receptor, the downstream target BIN2 is inhibited to release BZR1 and BES-1 to induce BR-responsive gene expression (Peres et al., 2019). It has been recently shown by our group that a BR derivative, 24-epibrassinolide (EBR) has a p53-independent apoptotic effect

* Corresponding author at: Istanbul Medeniyet University, Faculty of Engineering and Natural Sciences, Department of Molecular Biology and Genetics, Uskudar, 34700 Istanbul, Türkiye.
E-mail address: pinar.obakan@medeniyet.edu.tr (P. Obakan Yerlikaya).

https://doi.org/10.1016/j.biocel.2022.106360
Received 16 September 2022; Received in revised form 19 December 2022; Accepted 27 December 2022
Available online 29 December 2022

via altering polyamine metabolism and mainly inducing endoplasmic reticulum stress by targeting calreticulin in various cancer cells (Coskun et al., 2015; Obakan-Yerlikaya et al., 2017; Obakan et al., 2015).

Unfolded protein response (UPR) followed by endoplasmic reticulum (ER) stress is controlled by 3 membrane located receptors; IRE1alpha, ATF6, and PERK. These proteins transduce the signal of UPR to the nucleus by specific cascades to prevent ER stress-related cell death or promote it (Almanza et al., 2019). In resting conditions, all the stress sensors in the ER membrane are interacting with BiP/Grp78, however accumulation of un/misfolded proteins, sepatares BiP from the sensors. This phenomenon induces either their oligomerization and signaling; for IRE1 and PERK; or the transport to Golgi; for ATF6; to be cleaved and activated by proteases S1P and SP2 to initiate the transcription factor role (Bravo et al., 2013). Following autophosphorylation of IRE1aplha, a transcription factor called XBP1 gets alternative splicing and translation process and this activity change promotes chaperone proteins to induce ERAD. IRE1alpha also activates ASK1, JNK, and p38-MAPK to induce different pathways. One of the key protein that has various roles in both cell survival and cell death is called JNK and is regulated by the heterodimerization of a specific peer like Bim or Bcl-2 proteins (Junjappa et al., 2018). With the autophosphorylation of PERK protein, eIF2alpha is phosphorylated by serin51 and stabilizes the translation process by inhibiting or slowing down the process to prevent the accumulation of unfolded and misfolded proteins. PERK activation also promotes selective ATF4 activity and NRF phosphorylation by disrupting heterodimerization of NRF2 and KEAP1. ATF4 also promotes CHOP protein that induces apoptosis which is known as an er-stress-related apoptosis inducer (Liu et al., 2015). ATF6 has 2 different splicing regions called SP1 and SP2 and cleaved by Golgi apparatus. Cleaved ATF6 acts as an activated transcription factor and promotes ER-stress-related chaperones (Hillary and Fitzgerald, 2018). Therefore we previously demonstrated EBR induced ER-stress regardless of the p53 mutation status of various colorectal cancer cells (Coskun et al., 2015). In addition, our studies showed that EBR does not affect normal epithelial cells as an important outcome of our previous study was obtained in terms of its usefulness in in vivo experimental set-ups (Adacan and Obakan Yerlikaya, 2020). Therefore, we also evaluated the autophagic response in both in vitro and in vivo in this study.

Autophagy is a conserved process required for cellular homeostasis and prevention of nutritional, metabolic, and infection-mediated stresses by recycling damaged, non-functional proteins, organelles, lipids, nucleic acids via lysosome-mediated degradation (Kim and Lee, 2014). Autophagy process varies significantly in cancer cells. Depending on the type, mutations, and cellular content, autophagy protects tumor cells from stress-related cell death responses by mitigating or degrading related content. That leads to chemoresistance profiles in various types of cancers (Li et al., 2019). On contrary, prolonged autophagy can lead to cell death which is known as programmed cell death 2 (PCD2) (Linder and Kögel, 2019). Autophagy can be investigated in 3 different pathways which are known; macroautophagy, microautophagy, and chaperone-mediated autophagy. Therefore, we focus our research on macroautophagy-related pathways. Macroautophagy can be activated by AMPK in starvation-related conditions by disassociating the mTORC1 protein complex. AMPK phosphorylates ULK-1 which leads to disassociation of the complex (Fig. 1). Activated ULK-1 induces Beclin-1 dependent autophagic response (Kim et al., 2011). Under homeostasis, Beclin-1 stays heterodimers with Bcl-2 prevent activation of nucleation. Under stress conditions, Beclin-1/Bcl-2 heterodimers disassociated by JNK1 to eliminate the accumulations of stress factors by autophagy This process is known as the Nucleation of the autophagosome membrane (Marquez and Xu, 2012). There are various well-understood ATG proteins. These proteins interact between them and eventually form the ATG5-ATG12-ATG16L1 complex that leads to the Elongation process of the autophagosome membrane (Fig. 1). ATG7 protein is well known and essential for macroautophagy. ATG7 forms the ATG5-ATG12 complex and by interacting with ATG3 these proteins cleave LC3 to its active form to initiate the maturation process of the autophagosome (Wesselborg and Stork, 2015). p62/SQSTM1 marks the cargo that will be loaded in the autophagosome for degradation. (Liu et al., 2016) (Fig. 1). Following the maturation of the autophagosome, related content set off for degradation by fusing with the lysosome to form an autolysosome. Our previous studies enlightened that EBR could trigger autophagy in response to EBR treatment in both normal epithelial and colon cancer cells in vitro to cope ER stress (Adacan et al., 2020; Adacan and Obakan

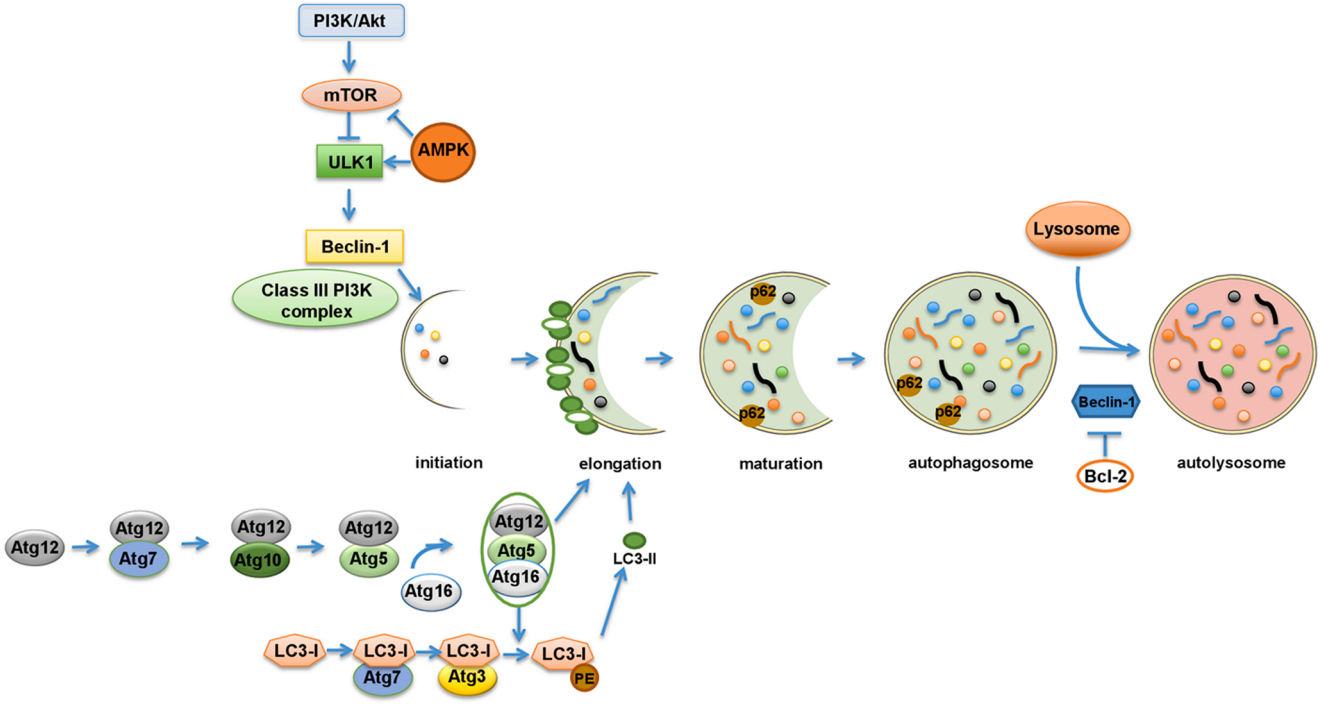

Fig. 1. The autophagy signaling pathways.

Yerlikaya, 2020). on the other hand, excessive activation of this process leads to the degradation of essential molecules for cell survival which is known as autophagic cell death. Recent findings suggest that autophagy can directly regulate cell death depending on the death stimulus, cell type, and context. The interplay between apoptotic cell death and autophagy is quite complicated and several apoptotic proteins are having role during this processes including caspases and Bcl-2 family members (Chen et al., 2019). For instance, caspase-9 and − 3 have been shown to inactivate ATG5 and Beclin-1 to initiate autophagy (Wirawan et al., 2010). Similarly, Bcl-2, Bim and Bax proteins are also interacting partners of Beclin-1 to coordinate the balance between autophagy and apoptosis (Kale et al., 2017; Lindqvist et al., 2014). Since cancer is basically a disease of uncontrolled cell division, the development and the progression is strictly linked to changes in the activity of cell cycle regulators, cyclins and cyclin-dependent kinases (CDKs). Both apoptosis and autophagy show a considerable correlation with the stress-related cell cycle responses. Therefore we also evaluated the expression levels of cyclins and CDKs in colon tumors excised from SW480 cells bearing SCID mice.

Cancer cell proliferation depends on the continuous activation of the cell cycle phases, G1, S, G2/M which is driven by cyclin-dependent kinases (CDKs) and their counterparts, cyclins. The CDK4 and CDK6 by the association of cyclinD1, D2 and D3, drive cell cycle progression from G1 into S phase, during which DNA replication occurs (Canavese et al., 2012). On the other hand, p16 and p21 are the negative regulators of the cycle (Ding et al., 2020). During S phase CDK2 forms a complex with cyclinA2 to exhibit progression. Finally the activation of cyclinB1 in complex with CDK1 is in charge during G2 phase of the cycle. All the mentioned proteins are targeted for the inhibition of cancer cell proliferation.

Our results showed that EBR, as suggested by our group as an apoptotic inducer, was able to induce autophagy in SW480 and DLD-1 colon cancer cells in vitro via the upregulation of Atg5–7, Beclin-1 expressions, and LC3 lipidation. In addition, the decrease in the expressions of p62 and Bcl-2 also show support the autophagic induction. The 3D cell culture results showed that EBR treatment was able to diminish spheroid diameter and altered the expression profiles of claudin, e-cadherin and β-catenin. We next subcutaneously administered SW480 cells to SCID mice in matrigel and treated with daily dose of increasing EBR concentrations (0–720 μg/kg) for two weeks. EBR treatment was able to reduce tumor volume and diameter, inhibiting the cell cycle progression. We also observed that mice treated with EBR exhibited a downregulation in mTOR and p62 expressions and mTOR phosphorylation, suggesting that autophagic induction occurs. Interestingly, no ER stress induction was observed in tumor samples generated with SW480 inoculation. BiP/Grp78 and CHOP expressions were higher in untreated tumor samples correlated with the poor prognosis of SW480 bearing SCID mice. Finally, we conclude that EBR treatment was able to stop the tumor progression in mice bearing an aggressive tumor model and induces cytostatic responses rather than a cytotoxic response in vivo.

2. Materials and methods

2.1. Cell Culture

Colon cancer cells SW480 (ATCC # CCL-228) and DLD-1 (ATCC # CCL-221) were cultured at 37 °C in a humidified 5% CO2 incubator (HERAcell 150; Thermo Electron Corporation, Waltham, MA, USA). DLD-1 cells were grown in McCoy's 5 A medium (PAN Biotech, Aidenbach, Germany), SW480 cells were grown in MEM medium (PAN Biotech). All media were supplemented with 10% fetal bovine serum (PAN Biotech) and 10000 U penicillin/ml, 10 mg streptomycin/ml (PAN Biotech). EBR (CAS 78821-43-9) was purchased from Apollo Scientific. It was prepared at a stock concentration of 5 mM. EBR was used at a final concentration of 30 μM in vitro studies which was proved by our group as the apoptotic concentration in our recent articles. For in vivo studies, EBR was prepared with DMSO as the solvent and mice treated with increasing concentrations of EBR (0–240–480 and 720 μg/kg). It was completed with saline to 200 μl final volume and prepared in 500 μl syringes. Injections were performed into the peritoneal area of SCID mice and repeated daily for 15 days.

2.2. Cell Viability Assay

SW480 and DLD-1 cells were seeded into each well of a 96-well petri dish at a density of 1×10^4 cells, and the cells were incubated in a 37 °C in a CO2 incubator. Cells were treated with 30 μM EBR for 12, 24, and 48 h. At the end of the incubation, 5 mg/ml of 3- (4,5-dimethyltriazol-2-yl)-2,5-diphenyltetrazolium bromide (MTT) agent was added and cells were incubated at 37 °C for 4 h. The resulting formazan crystals were solubilized in 200 μl dimethyl sulfoxide (DMSO). The microplate was measured in ELISA reader for the absorbance rate at two wavelengths at 570 nm and 655 nm.

2.3. Wound Healing

SW480 and DLD-1 cells were seeded at 5×10^4 cells in a 35 mm petri dish to obtain morphology overnight. The next day, the cell monolayer was wounded with a 200 μl pipette tip and the wound width was measured under light microscope. Untreated and treated samples with 30 μM EBR were incubated for 12, 24, and 48 h. The wounds were observed under the microscope and the widths were measured daily after incubations. After the measurement, the fixed cells were stained with crystal violet (0.5% w/v crystal violet, 25% methanol) at room temperature (RT) for 40 min, and the results were confirmed under the light microscope.

2.4. Fluorescence Microscopy

Cells were seeded at 1×10^4 cells in a 6-well petri dish and incubated overnight. Cells were treated with 30 μM EBR for 48 h.

2.4.1. 4′,6-diamidino-2-phenylindole (DAPI) staining

The medium was replaced with the fresh medium containing 5 mg/ml DAPI and incubated for 10 min. The dye bound to the DNA was visualized under the fluorescence microscope at 350 nm excitation and 420 nm emission.

2.4.2. 3,3′-dihexyloxacarbocyanine iodide (DiOC6) staining

The medium was replaced with the medium containing 400 nM DiOC6 and incubated for 15 min. Cells with healthy mitochondrial membranes were displayed as green at 488 nm excitation and 525 nm emission at the end of the incubation period under the fluorescence microscope.

2.4.3. Acridine orange staining

The medium was replaced with the fresh one containing 2 mg/ml acridine orange. Acridine orange emits green fluorescence (520 nm) when bound to dsDNA that can pass through the cell membrane, and orange fluorescence (650 nm) when it stains ssDNA, RNA, or acidic compartments. After 10 min of staining, the media was changed and the cells were observed under fluorescence microscopy. Colon cancer cells were kept in an FBS-free medium for 2 h as a positive control and a starvation cell model was established.

2.4.4. Monodansylcadaverine staining

The medium was replaced with a fresh one containing 0.05 mM MDC. MDC specifically accumulates in regions containing lysosomal enzymes, acid phosphatase, and cathepsin D. The media containing MDC was changed after 10 min and observed under the fluorescence microscope. Colon cancer cells were kept in an FBS-free medium for 2 h as a positive control and a hungry cell model was established.

2.5. Spheroid on agar

1% agarose gel was poured into 96 Petri dishes and allowed to jell. SW480 and DLD-1 1×10^4 cells were seeded in a petri dish with and without 30 μM EBR in a final volume of 50 μl without contacting the agar. 1x PBS was added surrounding wells to prevent evaporation. The spheroid structure was examined the next day. According to the experiment plan, incubation was performed for the desired time, and imaging was performed under the microscope.

2.5.1. Hanging drop

SW480 (ATCC CCL-228) and DLD-1 (ATCC CCL-221) cells were seeded on the lids of 60mm2 Petri dishes at 1×10^3 cells in 20 μl medium. For EBR treatment, 1×10^3 cells were prepared in a medium containing 30 μM EBR in a final volume of 20 μl and seeded onto a 60mm2 petri dish. 10 ml PBS is added into the Petri dishes and carefully covered. Petri dishes were incubated at 37 °C, 5% CO2, overnight. According to the experiment plan, incubation was performed for 24 and 48 h, and imaging was performed under the microscope. The experiment was repeated at least 20 times.

2.5.2. Spheroid staining

DiOC6 and DAPI dyes were prepared at 2x concentrations in a final volume of 50 μl for the spheroid cell model and 20 μl for the hanging drop cell model. In the spheroid cell model, they were carefully added to the Petri dishes without contacting the medium, and after the incubation period for each dye, spheroids were visualized under the fluorescence microscope. In the hanging drop model, dyes were slowly added to the side of the drop without disturbing the drop structure and incubation was performed in a time-varying according to the dyes. After incubation, imaging was performed under the fluorescence microscope for required excitation and emission wavelengths.

2.5.3. Colony Formation Assay

Colon cancer cells SW480 and DLD-1, were seeded at 1×10^4 cells in a 6-well petri dish and incubated overnight for attachment. 30 μM EBR was applied to the cells. After 12, 24, and 48 h of drug administration, cells were replaced with fresh media. The media in the wells were removed after 14 days, washed with 1xPBS, and incubated for 5 min with a 3:1 ratio of methanol: acetic acid for fixation. After the fixation, cells were stained with crystal violet and visualized under light microscope.

2.5.4. Protein Isolation and quantification

1.5×10^5 SW480 and DLD-1 cells were seeded in 100 mm2 Petri dishes. The cells were then kept in the incubator following 30 μM EBR treatment for 12, 24, and 48 h. Later, cells were collected from the Petri dishes by a scraping method using 1x PBS solution and precipitated by centrifugation at 16,000 g for 2 min. This process is repeated until all the cells in the Petri dish were collected and precipitated. Lysis buffer was added to the cells following the removal of the supernatant. The samples were incubated for 20 min at RT in a shaker and then centrifuged at 16,000 g for 20 min at + 4 °C. The supernatant was taken into a new microcentrifuge tube and stored at − 80 °C as the total protein isolates. PhosSTOP™ (Sigma Aldrich, Schnelldorf, Germany) was used for the detection of phosphorylated proteins. Protein quantification was carried out using the Bradford method, and a standard curve was first constructed using increasing amounts of Bovine Serum Albumin (BSA). 1 μl of each sample was added and 200 μl of Bradford solution was added on it and left in the dark for 5 min. The samples were read in a microplate reader at 595 nm wavelength. Protein concentration values were obtained by using the absorbance values formed.

2.5.5. Westernblotting

For the immunoblotting technique, the isolated proteins were mixed with Laemmli (5X) loading buffer and 40 μg protein samples were prepared by keeping them at 95 °C for 5 min. Then, the protein samples were loaded into 12% acrylamide/bisacrylamide gels at the specified concentrations. Following the running step, protein samples were transferred to the polyvinyl fluoride (PVDF) membranes activated by methanol. After the transfer process, the membranes were kept on a shaker in 5% skim milk powder (1xTBS containing 0.1% Tween 20) at RT for 1 h. Membranes were kept at + 4 °C overnight in the selected primary antibodies prepared at a ratio of 1:1000 (Cell Signaling Technologies). After the primary antibody labeling, the membranes was washed with 1xTBS-T solution three times for 5 min before being incubated with the secondary antibodies. Following overnight incubation with the secondary antibodies (1:3000), the membranes were washed with TBS-Tween solution twice for 5 min and with TBS solution once for 5 min. Membranes were treated for 2 min with chemiluminescence solution and the signals from the HRP conjugated secondary antibodies were detected using Chemidoc MP Imaging system (Bio-Rad Laboratories, Hercules, CA). All results were repeated at least three times and the representative blots were given. All antibodies were purchased from Cell Signaling Technology.

2.5.6. Immunofluorescence

Cells were seeded on poly-D-lysine coated coverslips at a density of 1×10^4 cells/well. After 30 μM EBR treatment, the medium was discarded and cells were washed 3 times with 1x PBS. Then, 1 ml methanol was added and the samples were incubated for 10 min at RT. After the methanol removal, the coverslips were allowed to dry and washed 3 times with 1x PBS. Then, 1 ml Triton X-100 solution was added to the samples and were subjected to 15 min incubation at RT, washing step was performed 3 times with 1x PBS. After washing step, 1x PBS solution containing 0.5% BSA (PBB) was added 3 times, and incubated for 45–60 min with 1 ml of PBS solution containing 2% BSA (BLOCK) at RT (10–15 rpm). The prepared primary antibody was placed on the coverslips. The well was covered with a tightly wet filter paper, covered with foil and incubated overnight on a shaker at 4 °C at 10–15 rpm. The next day, coverslips were washed with 500 μl PBB solution 3 times, DAPI was added to the prepared secondary antibody and added into the wells, Wells were covered with a wet filter paper and covered with foil. After the incubation period for 60 min on a shaker at 4 °C at 10–15 rpm. Following 3 washing steps with 500 μl PBB solution, a drop of 1x PBS was dropped on the slides, and coverslips were covered with the cells at the bottom. The coverslips were transferred to the wells, facing upwards, and 1 ml PBS were added to each wells. A stretch of wet filter paper was placed on wells, covered with foil, and can be stored at 4 °C until light microscopy investigation.

2.6. 3D Cell Culture

96-well Petri dishes were used for 3D cell culture using BD Matrigel Matrix (356234). In 50 μl matrigel, 5×10^3 SW480 colon cancer cells were mixed with 50 μl MEM at a ratio of 1: 1 and placed in 96-well Petri wells in 4 repetitions for each condition. EBR was added to the wells where EBR was applied, with a total volume of 100ul in a total volume of 30 μM EBR in 50 μl cell mixture and mixed with matrigel at a ratio of 1: 1, and the final concentration was fixed. 1xPBS was added to the surrounding empty wells to prevent evaporation. Spheroid-forming cell populations were determined in the wells monitored by microscope every day, and spheroid sizes were checked every day. At the end of the 7th day, the experiment was terminated as the spheroids interacted with each other in the control group and reached a level that would affect the accuracy of the experiment.

2.6.1. Agar chemotaxis assay

1% and 0.6% agars were prepared and autoclaved. 2x FBS containing medium was prepared for bottom agar. 1% agar is cooled and mixed with 2x FBS containing medium at a ratio of 1:1 and 1.5 ml of the mixture is placed at the bottom of each well of 6-well petri dishes and

allowed to polymerize. For the top agar, 5×10^3 SW480 cells were mixed with 0.6% agar in 1.5 ml and added.

at the top of the bottom agar in a 1:1 ratio. In the conditions where EBR was added, 5×10^3 cells were added in 750 μl media containing 30 μM EBR and mixed with 750 μl of 0.6% agar. After the top agar is placed, they were incubated for 30 min at room temperature. After polymerization, samples were kept in a 5% CO_2 incubator at 37 °C. Later cells were visualized under the light microscope.

2.6.2. In vivo experimental set-up

The experiments were carried out at Acıbadem University, Transgenic Animals Laboratories, with the ethics committee approval (approval number: HDK-2019–34). A total of 18 female, two weeks age, severe combined immunodeficiency (SCID) mice were used in the experiments. Experimental groups were as follows: Healthy mice receiving EBR, tumor bearing control group, tumor bearing vehicle treated group, tumor bearing 240 μM EBR treated group, tumor bearing 480 μM EBR treated group, tumor bearing 720 μM EBR treated group. 7×10^6 SW480 colon cancer cells were inoculated with 200 μl of matrigel into the right limb cavities of mice. After 40-day incubation period, SW480 tumor sizes became visible in mice. Tumor sizes of the mice divided into groups were measured with the help of an electronic caliper every two days. The mice were weighed at daily intervals of 5 days before the daily EBR injections on the precision balance and their weights were noted. Before the mice were sacrificed, they were anesthetized with isofluorane and 500 μl of blood was collected from the jugular vein of the mice, and serum was preserved for further experiments. The mice were then sacrificed, their tumors were removed and their pictures were taken.

2.6.3. Protein isolation from tumor samples

T-PER Tissue Protein Extraction Reagent (78510) was used for protein isolation from tumors. Pieces taken from the tumors with a scalpel were cut into small sections on foil and weighed in tared microfuge tubes with a volume of 2 ml and homogenized on ice using a Dounce homogenizer, keeping the ratio of 1gr: 20 ml T-PER. Before T-PER was used, 1 tablet of complete, EDTA-free protease inhibitor cocktail (11836170001) was added in 10 ml. For phosphorylated protein isolation, the process was repeated up to this point and 1 tablet of protease inhibitor followed by 1 tablet of PhosSTOP (4906845001) tablet was added into 10 ml T-PER. After the homogenization process was completed, samples were centrifuged at 10,000 g for 5 min and the supernatant protein content was transferred to a separate 1.5 ml microfuge tube and stored at −80°C freezer.

2.6.4. ELISA

Human CEA ELISA Kit (Abcam, ab99992) was used for ELISA experiments. Blood samples obtained from mice were kept at room temperature for 30 min and blood was allowed to clot. Then the samples were centrifuged at 2000 g for 10 min. A visible difference between blood and serum was obtained and the serum was transferred to a new 1.5 ml microfuge tube. 50 microliters of serum samples were divided into new 0.5 ml PCR tubes with 2 replicates for each sample and completed to 100 μl final volume with Assay Diluent A provided by the kit. The recombinant human CEA standards provided by the kit were prepared by serial dilution technique as specified and diluted to at least three samples. The samples were added to the wells and incubated overnight at + 4 °C in a low-speed rotating incubator. The next day, washing steps were carried out 4 times with 300 μl 1x wash solution and 100 μl of 1x biotin-labeled CEA antibody was added to each well and incubated at low speed for 1 h at room temperature. The same washing steps were repeated after incubation. After washing, samples were incubated at low speed for 45 min with 100 μl 1x Streptavidin solution and were washed once more. Subsequently, TMB was added to a single-step substrate solution and incubated for 30 min at low speed in the dark. After incubation, 50 μl Stop solution was added and read at 450 nm. The results have been analyzed in elisaanalysis.com belonging to the company elisakit.com and the values have been interpreted.

2.6.5. Immunohistochemistry

The sections taken from the tumors were kept in 10% buffered formalin solution at 4 °C for 16 h. Samples washed with 70% ethanol every other day for 1 week were subjected to tissue follow-up after 1 week. In tissue follow-up, samples were kept in 70% ethanol for 10 min, with 80% ethanol for 20 min, then in 90% ethanol for 20 min, in 96% ethanol for 15 min, in 100% ethanol for 15 min, in 100% ethanol for 15 min, and then kept in xylol for 2 times for 5 min and 42- Transfer to 44 paraffin and let stand at 44 °C overnight. The next day, 58 paraffin transfers and tumor samples were incubated at 58 °C for 2 h. After incubation, the tissues were embedded in 58 paraffin and kept at room temperature for 1 week to harden. In the sectioning process, the paraffin blocks placed in the microtome were sectioned with a thickness of 4 micrometers, taken on prepared slides covered with poly-L-lysine in a water bath at 40 °C, and incubated at 37 °C overnight. The slides were taken into the chalet and kept 2 times in xylol for 5 min. Then, it was kept in 100% ethanol for 2 times 5 min, in 95% ethanol for 2 times 5 min, in 70% ethanol for 2 times 5 min and it was kept in dH2O for 5 min. For antigen enhancement technique, slides were placed in a special heat-resistant container and the container was filled with 10 mM citrate buffer and boiled in the microwave for 15 min. Then, the slides were washed for 10 min with a washing buffer consisting of 50 mM tris + 0.01% tween20. After washing, it was treated with 1.5% H2O2 prepared in methanol for 15 min. Slides treated with the blocking solution contained in the Noves HistoStain Plus kit for 10 min were coated with Ki67 prepared with a dilution of 1:100 and cytokeratin18 was prepared with a dilution of 1:200, and covered with a slider-sized parafilm. The closed slides were kept at 4 °C overnight for primary antibody binding. The next day, the slides taken in the washing buffer were washed for 15 min, and the secondary antibody contained in the kit was added and waited for 30 min. After incubation, the slides kept in the washing buffer for 10 min were treated with Streptavidin peroxidase in the kit for 10 min. Afterward, the slides taken into the washing buffer were transferred to dH2O by waiting 10 min more. Slides treated with the AEC kit were allowed to wait for reaction time. By calculating the reaction time, AEC was applied to all samples for the same time and the reactions were terminated with H_2O. After finishing, the slides were covered with glycerol-vinyl-alcohol (GVA) Mounting Solution and covered with a lamel. Samples were visualized under the light microscope.

2.7. Statistical analysis

All the experiments were statistically analyzed by GraphPad Prism 6 software (http://www.graphpad.com/). Error bars in the graphs were generated using ± standard deviation (SD) values. A statistical significance test was utilized by using ANOVA Bonferroni's multiple comparisons test. $p < 0.05$ was taken as a level of significance. Results were repeated at least three times. The immunoblotting results shown are representative of three separate experiments.

3. Results

3.1. Epıbrassınolide treatment decreased cell viability in DLD-1 and SW480 colon cancer cells and altered Akt/mTOR/Ulk-1 signaling

We first examined SW480 and DLD-1 colorectal cancer cell viability following EBR treatment. Our results showed that 30 μM EBR decreased cell viability in a time-dependent manner for both cell lines (Fig. 2A). EBR treatment also induced autophagy within 48 h. In SW480 cells, pAMPK Thr172 was upregulated by 2 fold at 48 h, however, it was found downregulated in a time-dependent manner in DLD-1 cells. The active form of Ulk1 protein is represented by Ser555 phosphorylation (Fig. 2B). We found that pUlk1 Ser555 was increased after 24 h in SW480. In

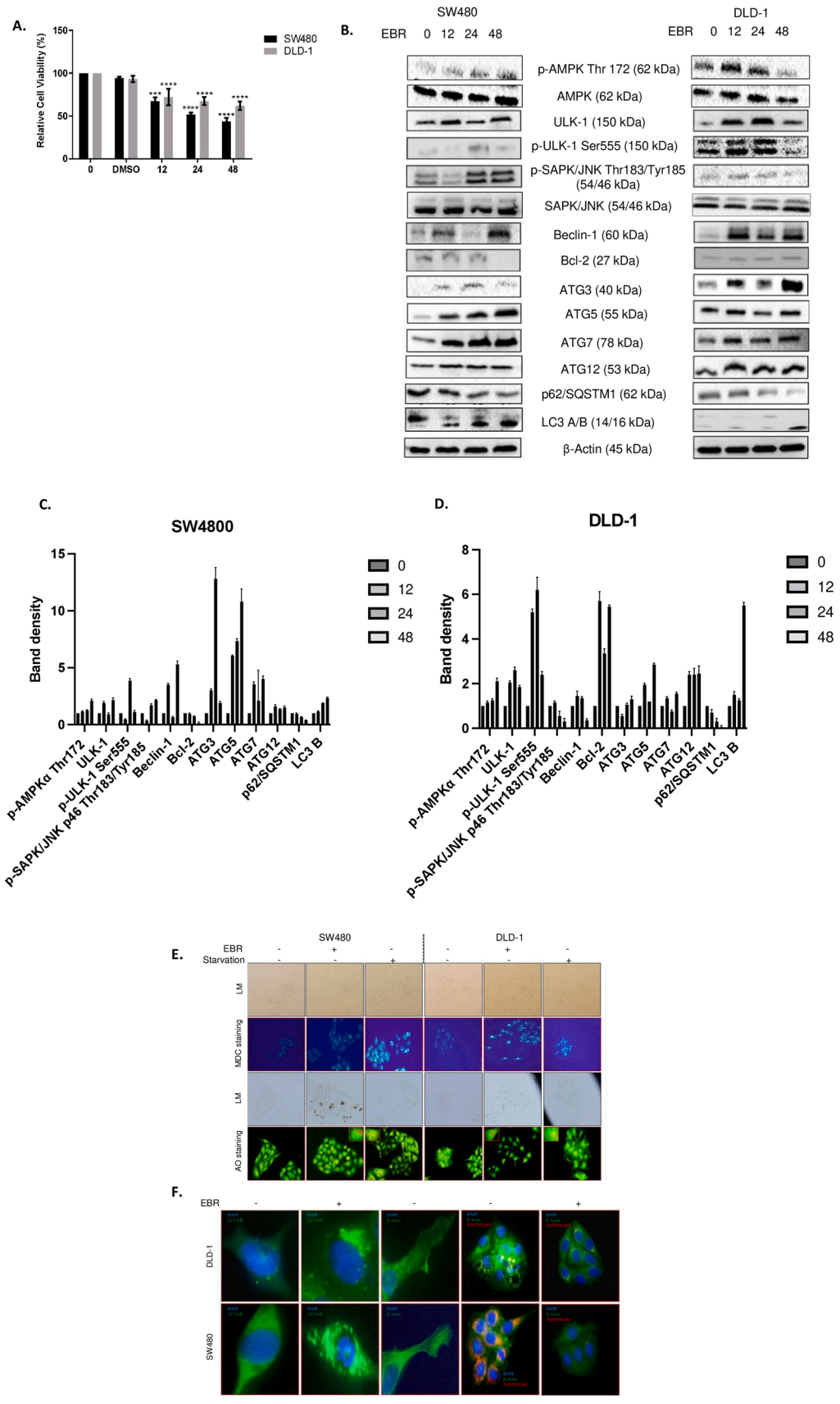

Fig. 2. EBR induced cell viability loss and caused autophagic induction in SW480 and DLD-1 cells. **A.** The effect of time-dependent EBR treatment (30 μM) on cell viability in SW480 and DLD-1 cells were determined by MTT assay. DMSO effect was also tested for both 24 and 48 h. * ** *$p \leq 0.0001$, * **$p \leq 0.001$ **B.** Total protein was isolated after time-dependent EBR treatment, and the expression profiles of autophagy biomarkers and upstream regulators were determined by immunoblotting using appropriate antibodies. β-actin was used as loading control. **C.** The densytometric analyses of the bands were given as column graphs for SW480 and **D.** DLD-1 cells. **E.** SW480 and DLD-1 cells were treated with EBR for 48 h. Autophagic and acidic vacuoles were labeled with monodansylcadaverine (MDC) and acridine orange (AO). LM: light microscopy, Magnification:20 × 10. **F.** Detection of LC3 and p62/SQSTM1 expression levels in EBR treated colon cancer cells for 48 h by immunofluoresence. DAPI was used to detect nucleus and the β-actin labeling was performed for the housekeeping expression. Magnification: 40 × 10.

contrast to SW480, EBR treatment induced pUlk1 Ser555 activity following 12 h in DLD-1 cells (Fig. 2B). pSAPK/JNK Thr183/Tyr185 also were upregulated in a time-dependent manner in SW480 cells. Conversely, the decreased phosphorylated protein expressions were observed in DLD-1 cells (Fig. 2B). We next examined the expression profiles of Bcl-2, since it is a critical protein which binds to Beclin-1, preventing its activity and removed by JNK protein. We found that Bcl-2 protein expression decreased in a time-dependent manner and more importantly completely abolished after 48 h of EBR treatment in SW480 cells (Fig. 2B). The expression of Bcl-2 in DLD-1 cells was only half decreased following 12 h EBR exposure, and became the same as control samples after 24 h. We also observed that both cell lines exhibited increased expression of Beclin-1 after both 24 and 48 h EBR exposure, suggesting that SW480 cells might have an increased upstream signaling for autophagy induction, and DLD-1 cells lost the upstream signaling throughout time. To understand the execution of autophagy, we checked ATG protein expressions and showed that all four major ATG proteins 3/5/7/12 were upregulated in both cell lines with a time-dependent EBR treatment (Fig. 2B). The lipidated form LC3 protein, LC3-B 2nd which represents the activation of autophagosome-related activity exhibited an increased expression at all time point applications of EBR in each cell lines. We also confirmed the autophagic activity by checking the expression profile of p62/SQSTM1. Fig. 1B clearly indicated that 30 μM EBR treatment able to downregulate time-dependently the p62/SQSTM1levels, proving that there are autophagosome-lysosome fusion and correct execution of autophagy (Fig. 2B). All the alterations in band densities were calculated with Graphpad Prism and given in Fig. 2C and D. The increase levels of monodansyl-cadaverine (MDC) and acridine orange staining also clearly showed that autophagic vesicles and more specifically acidic ones were increasing after EBR treatment for 48 h (Fig. 2E). We further examined the activation and execution of autophagy via immunofluorescence assays. The most crucial markers for autophagy known to be are LC3 and SQSTM1. The results of the immunofluorescence experiments are also positively correlated with the western blot results of these specific proteins. Upregulation of LC3 protein and downregulation of SQSTM1 protein expression observed with the immunofluorescence assay following 48 h of EBR treatment (Fig. 2F). Collectively, these results prove EBR-induced autophagy in DLD-1 and SW480 cells.

3.2. Epibrassinolide reduced the diameters of spheroids in both hanging drop and on-agar models of colon cancer cells

The 3D colon cancer models were generated by hanging drop and agar plates to show the anti-cancer potential of EBR before moving to the in vivo experiments. We observed shrinkage of the spheres following 24 and 48 h of 30 μM treatment in both experiments. The diameter of spheres were diminished compared to untreated samples as shown in Fig. 3A. We also stained the 3D tumor models with DiOC6 and DAPI, and showed that the mitochondrial membrane potentials are lost and the viable cell numbers decreased with the EBR exposure after 48 h (Fig. 3B). SW480 cells were picked for in vivo experiments, since they are much more sensitive to EBR than DLD-1 and defined as aggresive colon cancer model. Therefore we performed 21 days long spheroid assay to determine the 3D viability of the SW480 spheres following EBR treatment. As shown in Fig. 3C, SW480 spheroid has a diminished diameter and dark parts, possible necrotic cells, however they survived after 21 days of EBR treatment (Fig. 3C). Lastly, we used matrigel as a basement membrane matrix and formed 3D SW480 culture. Fig. 3D showed that EBR exerted a cytostatic effect in 3D in vivo mimicking environment (Fig. 3D).

3.3. Epibrassinolide treatment reduced wound healing without affecting the expression of EMT biomarkers

Next, we evaluated the mobility of SW480 cells, by an agarose chemotaxis assay. The upper part of the agarose mixed with a lower concentration of FBS, whereas the lower part with higher FBS concentration. The experiment was observed for 21 days. As seen in Fig. 4A, there were little fracture of cells showing positive chemotaxis to lower part of the Petri dish compared to untreated sample. Later, specific protein markers of cell mobility were determined via western blotting. Claudin-1 and E-cadherin expressions were downregulated following EBR treatment for 48 h. β-catenin expression was found downregulated following 48 h EBR treatment. However, no change was observed for vimentin expression level (Fig. 4B). To determine the mobility of SW480, we performed a scratch assay. Following EBR treatment, the mobility and the wound healing potential of the cells were decreased compared to after 48 h EBR treatment (Fig. 4C).

3.4. Intraperitoneal epibrassinolide administration reduced the overall tumor diameters and decreased the serum CEA levels in SCID mouse colon cancer xenograft model

Following 15 days of increasing concentrations of EBR treatment in SCID mice, tumor mass in diameters, and tumor volumes were drastically decreased (Fig. 5A). Representative images of tumors are shown in the figure (Fig. 5B). There were no changes observed regarding SCID mice weight after SW480 inoculation (Fig. 5C). Representative SCID mice images are shown in the figure (Fig. 5D). According to the data obtained from CEA ELISA, CEA concentration was not determined in the serum of mice without a tumor. However, 590 ng/ml CEA concentration were detected in the tumor control group and 720 μg/kg EBR administration lowered the CEA concentration to 12 ng/ml (Fig. 5E). Ki67 is also known as a marker of proliferation and coded by the *MKI67* gene. CK18 coexpressed with complementary partner CK8 and considered as a prognostic biomarker that is involved in both motility and tumor progression. Histological examination and the related graph showed decreased signals of Ki67 and CK18 antibodies following EBR treatment (Fig. 6A and B).

3.5. Endoplasmic reticulum stress and apoptotic markers were not induced in tumor samples after epibrassinolide administration while cell cycle is impaired

We next analyzed the expression levels of signaling pathways, autophagy and ER stress affected that we know from our previous studies. mTOR and pmTOR levels were downregulated following 720 μg/kg EBR treatment in tumor samples. There was no specific autophagy induction observed related to AMPKα phosphorylation. However, p62/SQSTM1 protein levels depleted following EBR treatment. There was no ER stress-related activation observed. However, BiP/Grp78 and CHOP levels were higher than expected in control tumors. Which can relate to poor prognosis and altered progression of control tumors (Fig. 6C). To further determine the role of EBR treatment in SW480 tumors, we examined other important cancer pathways, apoptosis and the cell cycle progression via westernblotting. There were no specific alterations observed of pro-apoptotic Bax, Bim, Caspase9, cleaved-Caspase3, and cleaved PARP expressions. However, Bcl-2 protein expression was downregulated following EBR treatment (Fig. 7A). In addition we observed that CyclinB1, CyclinD3, CyclinA2 levels were depleted after 720 μg/kg exposure of EBR to SCID mouse colon cancer model. Next, we also checked the expression of CDK4, CDK6, P21 Waf1/Cip1, and P27 Kip1 protein levels. We observed that CDK4 and CDK6 protein levels also depleted and P27 Kip1 specific cell cycle blocker protein upregulated drastically, rather than p21 (Fig. 7B).

All these findings suggest that, EBR is an apoptotic inducer in vitro and can act on different signaling pathways including ER stress and autophagy. The autophagy induction was seen in both aggresive forms of colon cancer representing cell lines SW480 and DLD-1. SW480 was found more vulnerable, despite the autophagic induction, which was supported by the 3D cell culture techniques aiming to show potential in

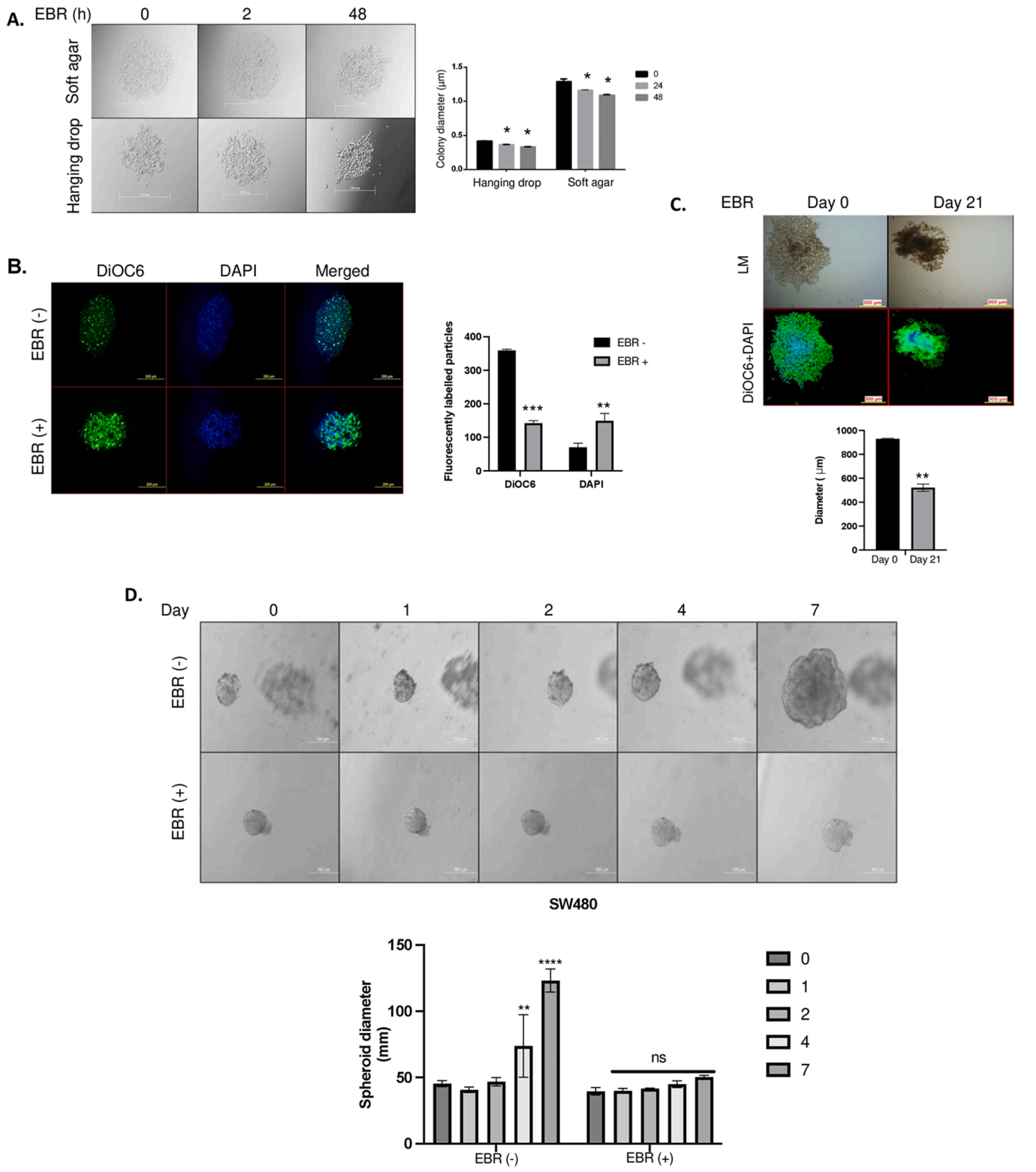

Fig. 3. EBR diminished colon cancer spheroid diameter and induced cell death in the spheroids. **A.** Soft agar and hanging drop techniques were perfomed to obtain spheroids. Time-dependent EBR treatment was performed and the spheroid diameters were calculated. Colon cancer spheroids on **B.** hanging drops and **C.** on soft agar were co-stained with DAPI and DiOC6 and the cell viability loss were visualized following EBR treatment. *p ≤ 0.05, * *p ≤ 0.01, * ** *p ≤ 0.0001. Magnification: 40×10 **D.** SW480 cells were grown in matrigel for a week in the presence or absence of EBR. The diameter of spheres were calculated and represented as a graph using Graphpad Prism. Magnification: 40×10.

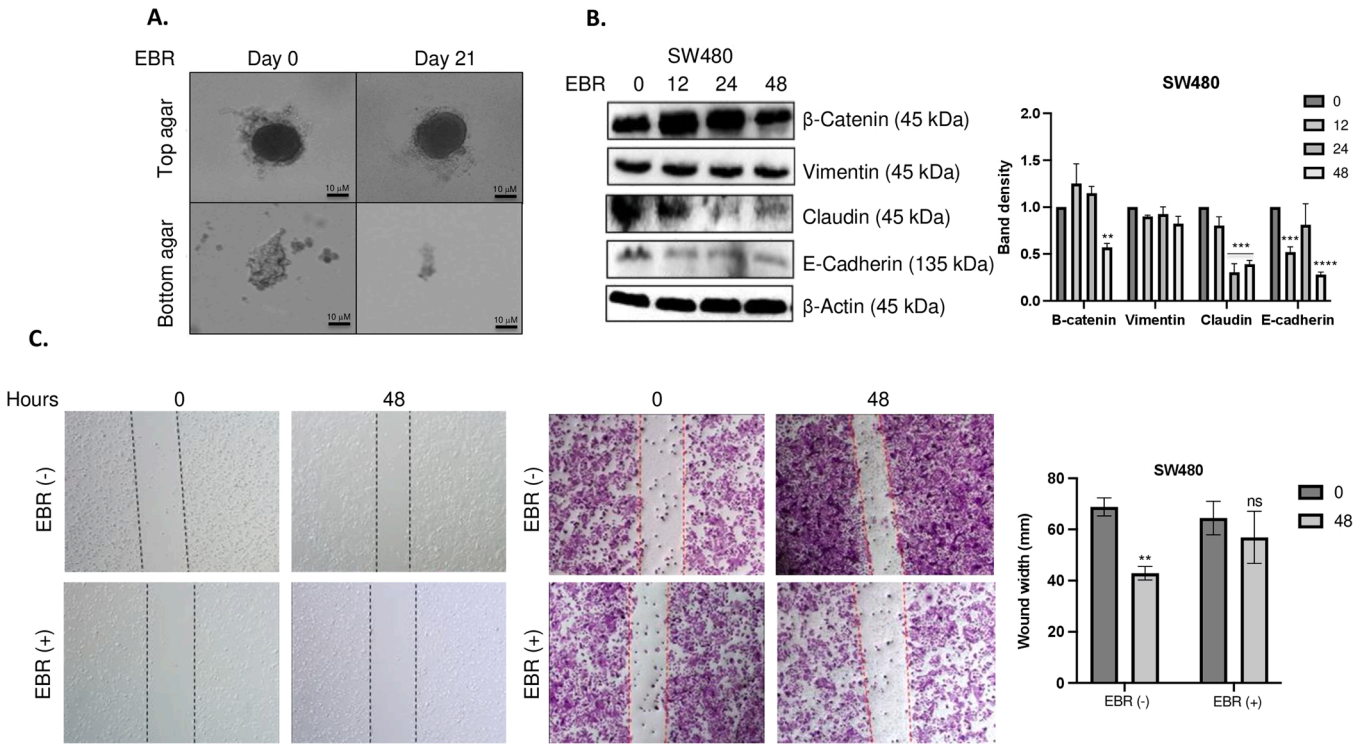

Fig. 4. EBR inhibited the invasion of SW480 cells. **A.** Agar chemotaxis assay was performed by using two different agar plates with various FBS concentrations. Cells were seed on the top agar and their chemotaxis behavior towards increased FBS containing agar was observed under light microscope. **B.** The expressions of proteins responsible from cell mobility were checked with immunoblotting with the appropriate primary antibodies. β-Actin was used as a loading control. **C.** 5×10^5 cells were seeded into 6 well plates. The wound healing assay was performed following EBR treatment 48 h. The wound closure was calculated by Olympus IX70 light microscopy. * *p ≤ 0.01.* **p ≤ 0.001,.* ** *p ≤ 0.0001. Magnification: 20 × 10.

vivo effects. When administered to SCID mice, SW480 cells generated colon cancer tumor and their diameters and mass have diminished following EBR administration. Despite the in vitro findings, EBR treatment in mice did not induce ER stress induction or autophagic regulation, however induced cell cycle arrest at 720 μg/kg concentration. In addition the inhibition of Ki67 and CK18 were suggested as promising effects of EBR. Taken together, EBR can be considered as a successful therapy model for colon tumors to activate cytostatic responses rather and cytotoxic ones.

4. Discussion

EBR is a BR member that acts as a growth hormone in plants. Due to the structure of EBR, it is emphasized that the molecular mechanism in mammals can be associated with steroid hormones. Although its molecular mechanism in plant cells was elucidated many years ago, studies on its molecular effects in cancer cells were relatively new. Many research groups demonstrated that EBR promotes cell cycle arrest as well as disrupts polyamine metabolism and induces ER stress-related apoptosis in colorectal cancer cells, prostate cancer cells, and breast cancer cells (Coskun et al., 2015; Kohli et al., 2020; Obakan et al., 2015). To understand the molecular targets of EBR, SILAC assay was performed by our group and obtained the result that EBR targets chaperone protein calreticulin and promotes ER-stress related pathways (Obakan-Yerlikaya et al., 2017).

In this study we aimed to show the anti-tumoral effect of EBR in colon cancer cells by 3D cell culture as well as in vivo SCID mouse model. SW480 and DLD-1 colorectal cancer cell lines that have different p53 profiles and both exhibited cell viability loss after 30 μM EBR in a time-dependent manner. We found that SW480 cell viability decreased below 50% following 48 h of EBR treatment. However, DLD-1 cells presented a robust profile compared to SW480. Our recent study also pointed the same situation with different p53 profiles (Coskun et al., 2015). Our previous study also demonstrated that EBR promotes PI3K/Akt-related pathways to induce autophagy and polyamine metabolism in SW480 and DLD-1 colon cancer cells (Adacan and Obakan Yerlikaya, 2020). We showed that the induction of autophagy were enlightened. We demonstrated that EBR disrupted energy metabolism and activated AMPK protein by Thr172 phosphorylation with this study. The first induction of AMPK was found at 12 h time period following EBR treatment in both SW480 and DLD-1 cell lines. However, while SW480 cells kept the signaling through AMPK, DLD-1 cells decreased the signaling at 48 h. Regarding this result, we might conclude that both cell lines deprived of energy following EBR treatment and tried to replenish it by autophagy through AMPK protein (Willows et al., 2017). Activated AMPK phosphorylated ULK-1 at Ser555 and promoted ULK-1 regulated autophagic signaling by disassociating mTORC1 in both early time and late time treatment in DLD-1 and SW480 cell lines. However, DLD-1 cells kept the signaling at a 24 h time point to survive from initial stress. Even though ULK-1 protein upregulation means autophagic induction, the phosphorylated form of ULK-1 increased in 24 h time point in SW480 cells. This indicates that SW480 survived from the initial stress by other chaperon proteins for the alternative extinguishing method (Hardie, 2011). Highly altered JNK expression disrupts Beclin-1/Bcl-2 heterodimerization by phosphorylating Bcl-2 protein to mark it as cargo for degradation. SW480 depleted Bcl-2 expression is positively correlated with JNK phosphorylation after 48 h EBR treatment. Bcl-2 expression levels were upregulated following JNK depletion which can be correlated with the extinguishing of EBR related stress and the need for autophagic signaling (Dai et al., 2013). JNK is also known as a cross-talking protein that promotes various pathways (Shen et al., 2003). Following initiation of nucleation, ATG proteins are involved in forming the autophagosome for cargo degradation. ATG3, ATG5, ATG7, and ATG12 actively work in the nucleation and elongation process (Arakawa

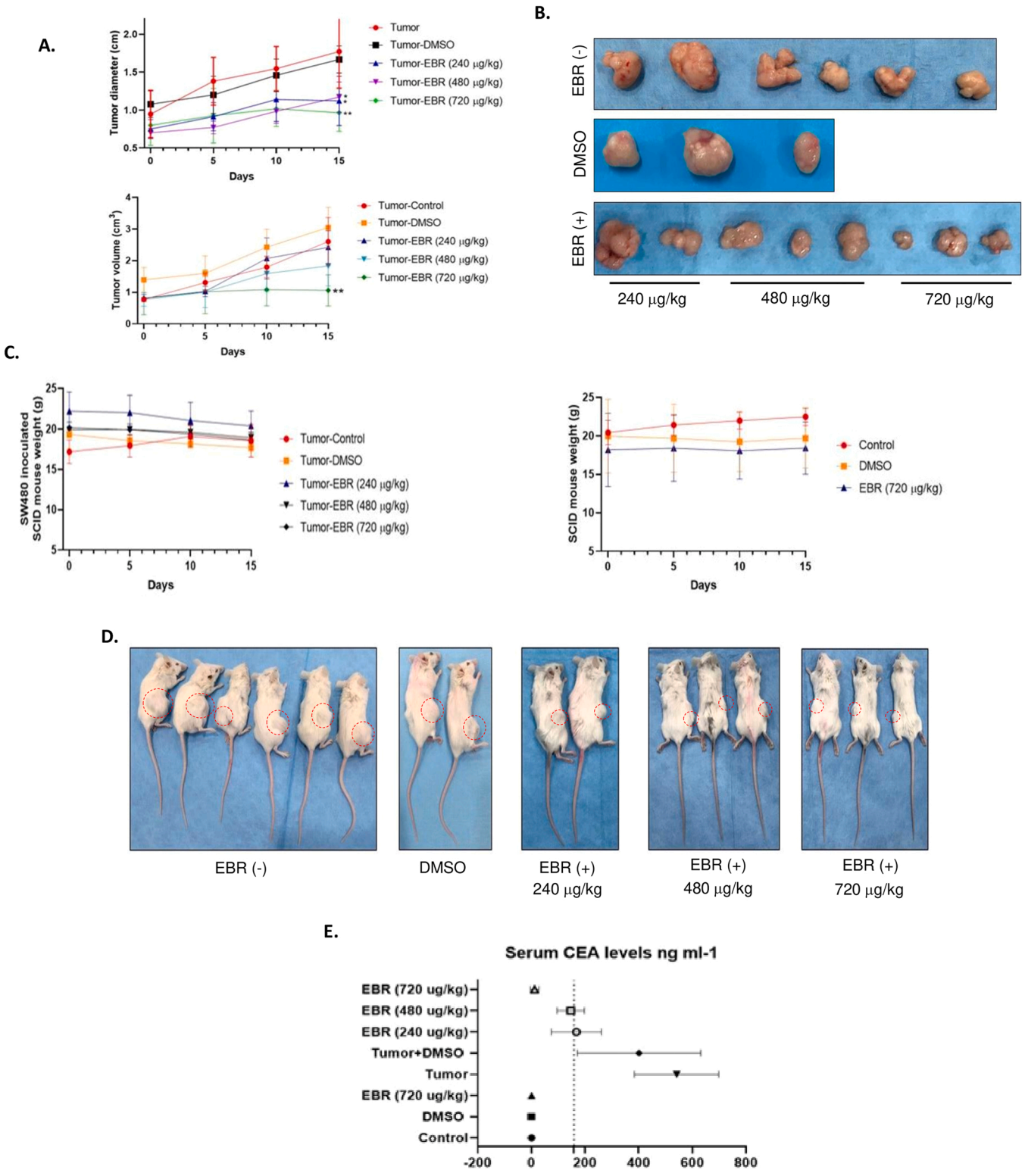

Fig. 5. EBR treatment diminished tumor size and volume without causing any significant health problem in non-treated SCID mice. **A.** SCID mice were treated with increasing concentrations of EBR (240, 480 and 720 μg/kg EBR) via intraperitoneal administration (daily for two weeks). DMSO group was used as control. Both tumor sizes and volumes decreased compared to untreated controls significantly in a dose-dependent manner. **B.** Representative pictures of the SW480-derived xenograft tumors with dose-dependent or without EBR administration for two weeks, were harvested from mice. The body weight of EBR administered mice in **C.** SW480-derived xenograft tumor bearing mice and control group without tumor formation was measured twice per week. The graph shows that the treatments did not have side effects on body weight of the mice. Data are shown as mean ± SEM. **D.** Representative pictures of the SW480-derived mice treated vehicle (DMSO) and dose-dependent EBR after two weeks. **E.** The serum CEA levels of EBR administered tumor bearing mice with or without EBR administration were determined by ELISA. * *$p \leq 0.01$.* **$p \leq 0.001$,.* ** *$p \leq 0.0001$.

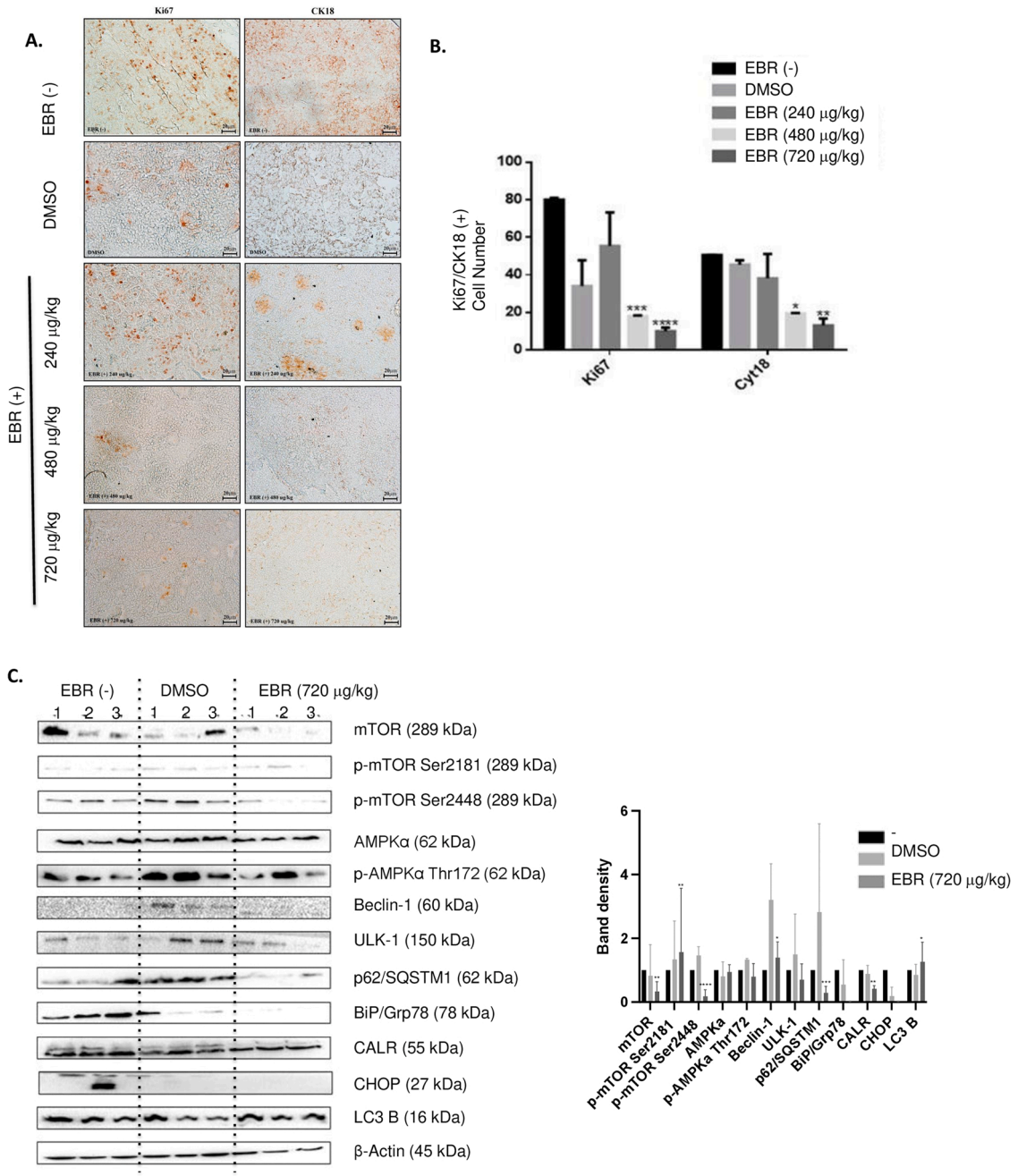

Fig. 6. EBR administration decreased Ki67 and CK18 expressions in SW480-derived xenograft tumors. **A.** The expression levels of Ki67 and CK18 were determined in control, vehicle and dose-dependent EBR administered SW80-derived xenograft tumors after resection via immunohistochemistry. Magnification: 20 × 10 **B.** The significant changes in the number of Ki67 and CK18 positive cells were given as column graph. Data are shown as mean ± SEM. * *p ≤ 0.01.* **p ≤ 0.001,. * ** *p ≤ 0.0001. **C.** Autophagy and ER stress biomarker expressions in tumors were determined with immunoblotting with the appropriate primary antibodies. β-Actin was used as a loading control.

et al., 2017). All the stated ATG proteins upregulated in both SW480 and DLD-1 cells in a time-dependent manner and promoted lipidation of LC3 protein. However, ATG5 and ATG7 are not necessary to finalize autophagy. In our previous study, we showed that EBR can promote an ATG5/7 independent pathway of macroautophagy in ATG5 -/- MEF cells (Adacan et al., 2020). p62/SQSTM1 accumulated following EBR treatment indicates that cells were tagging cargo molecules to promote intense autophagy to delay stress-related cell death. In both SW480 and DLD-1 cell lines, p62/SQSTM1 depleted in 48 h, and this result might be correlated with autophagic cell death in addition to survival benefits (Tsai et al., 2012). This intense autophagic signaling following 48 h EBR treatment also determined with immunofluorescence assays of both LC3-II and p62/SQSTM1 to indicate the morphologic advances following autophagy. The results also prove the autophagic termination was happening after 48 h treatment like Itakura et al. suggested the same profiles for macroautophagy termination (Itakura and Mizushima, 2011). Our previous research demonstrated that EBR promoted ER-stress-related cell death in both SW480 and DLD-1 cells. Puissant et al. recently suggested that autophagosomes might keep fusing with lysosomes to form autolysosome even though there was stress-related cell death. Based on this information, we also suggest that there might be a positively correlated cell death mechanism following both apoptosis and autophagy to promote autophagy-related cell death (Puissant et al., 2010). This is not the case at a 12 h time point, however,

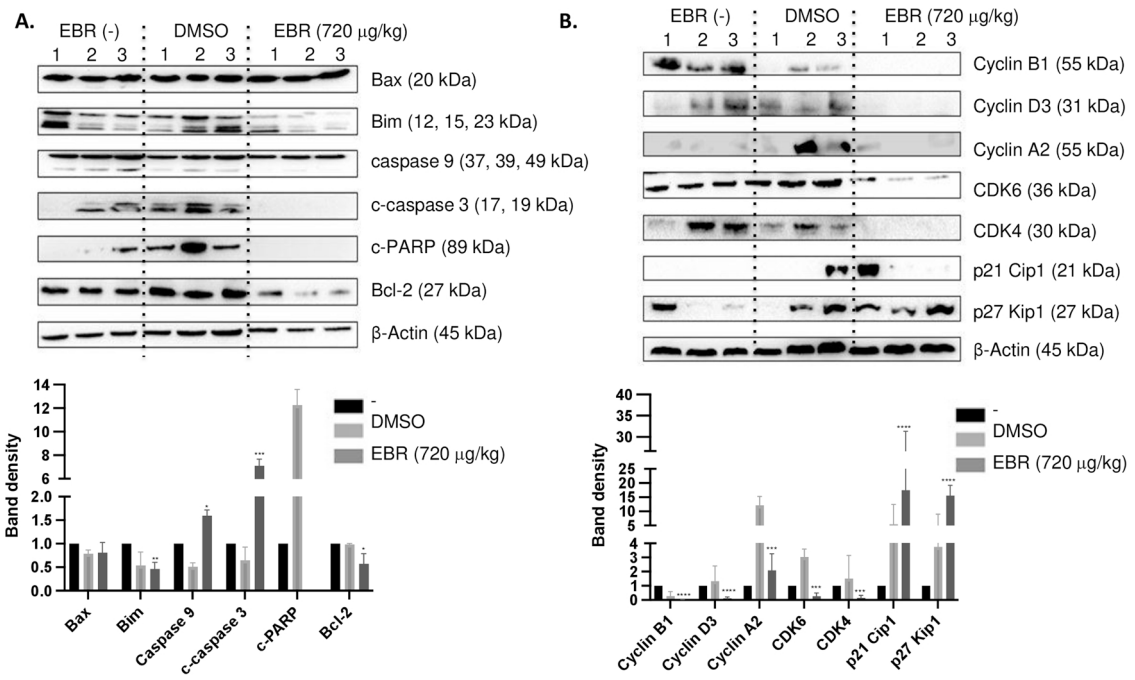

Fig. 7. EBR induced cell cycle arrest in SW480-derived xenograft tumors. **A.** The expression profiles of apoptotic and **B.** cell cycle proteins were investigated by immunoblotting using indicated primary antibodies. β-Actin was used as loading control. The band densities of at least three independent results were calculated using ImageJ and the graphs were generated using GraphPad Prism. Data are shown as mean ± SEM. *p ≤ 0.05, * *p ≤ 0.01.* **p ≤ 0.001,.* ** *p ≤ 0.0001.

it is clear that both DLD-1 and SW480 cell lines induced autophagy to remove excessive stress caused by EBR (Ogata et al., 2006).

Due to the more sensitive response, and still represents an aggresive colon tumor model, we decided to perform further 3D cell culture and in vivo experimental set-up with SW480 cell line to evaluate EBR potential action to diminish tumor size and volume. We performed two different 3D mimicking cell culture techniques and showed that EBR treatment for 48 h decreased the spheroids sizes compared to control samples. Studies using 3D cell culture techniques revealed that there were various protein alterations between 2D and 3D culture techniques in DLD-1, HCT116, and Caco-2 colon cancer cells (Riedl et al., 2017). To evaluate the viability we performed DiOC6/DAPI double staining on hanging drops and found that there was an increased amount of bright DAPI dots suggesting DNA cleavages following EBR administration. Although the effect was lesser than 2D on the same dose of EBR we observed DNA cleavages mostly in the edges as well as in the center of the spheroids. Teroxirone is a steroid-structured drug used in the treatment of lung cancer spheroids and the same effect that steroidal drugs can easily penetrate 3D cell structures (Ni et al., 2018). 21 days of EBR treatment was evaluated to mimic the effect in vivo. Following the treatment, spheroids lost the integrity of the structure and decreased in diameter. Other researches also suggested that U2OS, NIH-3T3, HeLa, PA317, C2C12, SH-SY6Y, A549, and 293 T spheroids also faced the same situation following cisplatin administration (Baek et al., 2016). Different colon cancer studies also suggested that another planted-derived ursolic acid administration decreased SW480, HT29, and HCT116 spheroids sizes, in fact, high dose administration was eliminated the formed spheroid (Lin et al., 2011). Administration of resveratrol and capsaicin also decreased SW480 spheroid diameters (McCubrey et al., 2017).

Our soft agar, wound healing, and colony assays showed that EBR had an intense effect in preventing cell division and mobility. Our western blot data of β-catenin, vimentin, claudin-1, and E-cadherin positively correlated with the mobility and cell division-related assays. Although E-cadherin decreased with EBR administration in a time-dependent manner, this result does not mean that cadherin alone can stabilize β-catenin while the rest of the degradation systems on the act (Jeanes et al., 2008). EGb761, a plant extract showed a positive correlation with our finding and prevented wound healing and invasion on SW480 and SW620 cells (Liu et al., 2017). Another study also suggests that sylibin and regorafenib combined administration prevented colony formation by targeting Akt signaling (Belli et al., 2017). Our previous work also showed that EBR can regulate Akt signaling to induce autophagy and cell death decisive mechanisms of the cell (Adacan and Obakan Yerlikaya, 2020). We further evaluate the 3D response of SW480 following EBR treatment by mimicking the 3D environment using matrigel. It's known that mimicking the 3D environment affects Akt and MAPK signaling pathways in SW480, Caco-2, DLD-1, HT29, LoVo, and Colo206F cells (Edmondson et al., 2014). Regarding our experiment, we demonstrated that when mimicking the 3D environment the same dose effect of EBR was altered and the known cytotoxic effect is converted to cytostatic effect.

After obtaining the tumor formation in SCID mice inoculated with SW480 cells, EBR was intraperitoneally injected consecutively for 15 days. Tumor sizes were measured and mice weighed every day. 720 μg/kg EBR effectively reduced the tumor size and volume compared to the lower doses of administration. However, EBR has a known lethal dose of 1000 mg/kg administration rate on mice (PCT/US2005/022780). We used a much lesser dose of administration to evaluate the effect. 240 μg/kg and 480 μg/kg dose administrations of EBR might be under the effective dose limit. When we look at the weights of mice in the absence of tumors, EBR and the vehicle did not affect mice weights. Although it looks like there were no significant changes in the weight of mice in the presence of tumors, mice lost weight to support tumor growth while tumor volume kept expanding (Murray et al., 1997). CEA is a well-known marker for cancer activity and can be detected in blood serum. We detected increased CEA levels in untreated tumor-positive blood samples compared to tumor absent samples. Therefore, we evaluated that CEA levels regardless of tumor absence w/wo EBR administration and demonstrated that 720 μg/kg EBR dose was effective enough to prevent CEA accumulation in blood samples of tumor positive mice. Other studies targeted various colon cancer types (LoVo, HCT116, HCT-15, HT-29, Caco-2, SW480, Colo205, HCT-6, LS180, Ls174T, and SK-CO-1) for decreased CEA expressions in response to chemotherapeutic drugs and modeled them using shRNA to elucidate the interaction

between CEA and TBRI (Li et al., 2010). Recent studies also showed that CEA and CEACAM1 are overexpressed in colorectal cancer cells and that high levels of CEA induce poor prognosis with liver metastasis and targeted this issue with anoikis as we did with EBR administration (Samara et al., 2007).

Ki67 is a proven marker of cell division and increased cytokeratin18 (CK18) expression followed by epithelial-mesenchymal transition and cell differentiation. Previous studies by other groups perfomed with EBR also demonstrated the cell cycle arrest in breast cancer cell lines (Steigerová et al., 2010). We found that 240 μg/kg EBR dose is non-effective since both CK8 and Ki67 signals increased following the administration. However, both 480 μg/kg and 720 μg/kg EBR administrations were able to decrease the Ki67 and CK18 signals. Autophagy in tumor samples was shown via westernblotting. We were able to detect p62/SQSTM1 degradation in tumor samples treated with 720 μg/kg EBR, however, there were no significant alterations detected including the initiation and pre-initiation phase proteins of autophagy such as mTOR, ULK-1, and Beclin-1. Earlier studies showed that p-mTOR levels can vary between regions of colon cancer tumors (Melling et al., 2015). Previous studies also determined that AMPK protein expression might have prognostic value in grade IV colorectal cancers and AMPK is specifically activated as a stress response to balance energy metabolism and disrupt cell cycle progression. The same study also suggests that AMPK protein activation has no value on cell survival-related signaling (Li et al., 2015; Suvorova and Pospelov, 2019). Therefore, without the alteration on specific initiation and pre-initiation proteins of autophagy and following p62/SQSTM1 degradation suggests that EBR induced ATG5/7 independent alternative macroautophagy pathway in mice (Nishida et al., 2009). In our previous work, we demonstrated that EBR induced ER stress in SW480 cells (Obakan-Yerlikaya et al., 2017). However, 720 μg/kg EBR administration had no such effect in vivo conditions. Recent studies suggest that BiP/GRP78 and CHOP are often upregulated, acting as a central stress sensor regarding the tumor microenvironment changes and related to poor prognosis (Wang and Kaufman, 2014). Regarding this issue, EBR inhibited tumor progression by diminishing CHOP and GRP78 protein levels. There was no pro-apoptotic induction observed following 720 μg/kg EBR administration. However, increased pro-apoptotic protein response was detected in control and vehicle samples. Increased caspase 3 activity promotes tumor differentiation and increased the volume of tumor (Hu et al., 2014). By decreasing the expression levels of caspase 3 and caspase 9, 720 μg/kg EBR administration negatively regulated aforesaid activity and presented a non-cytotoxic profile. Cyclins and CDKs as in charge molecules of cell cycle progression, therefore their negative regulator actions are in focus in many cancer mechanism (García-Reyes et al., 2018). CDKs having role in G1, S and G2 phases have been downregulated following 720 μg/kg EBR administration. Studies targeting CDKs and inhibitors in cancer cells showed that p27 protein interacted with cyclins that bound to CDKs and promoted degradation of the targeted complex (Ray et al., 2009). Previous studies on this field demonstrated that EBR downregulated cyclin D1, cyclin E, cyclin B1, CDK2, and CDK4 and simultaneously upregulated p21 and p27 cell cycle inhibitors in MCF-7, MDA-MB-468, LNCaP, and DU145 cancer cell lines (Steigerová et al., 2012). EBR treatment has also been shown to prevent cell cycle progression by decreasing retinoblastoma phosphorylation by other groups (Steigerová et al., 2010). EBR inhibited cell cycle progression by downregulating cyclins and CDKs and upregulated p27 Kip1 protein.

When we look at the plant-derived anti-cancer drugs that decreased viability and motility of the cancer cells, pomiferin was isolated from *Maclura pomifera* used as histone acetylase inhibitor, sulforafan was used as an epigenetic regulator of hTERT and simultaneously decreased mir-21 levels in HCT116 colon cancer cells (Martin et al., 2018; Son et al., 2007). In addition, timokuinon was isolated from *Nigella sativa* and inhibited COX-2 expression by altering prostaglandin E2 levels to prevent migration in both in vivo and in vitro (Hsu et al., 2017). Following these informations, EBR as a plant-derived steroid hormone-like anti-cancer drug has various stress-inducing capabilities in vitro, however, 720 μg/kg dosage of EBR has a cytostatic effect on SW480 tumors. EBR is known to have a 1000 mg/kg lethal effect in mice and dosage can be altered regarding this issue. Higher doses might have a cytotoxic effect and must be further tested for anti-cancer activity in vivo.

In conclusion, we demonstrated that EBR induced cytostatic responses in both 3D cultures and in vivo experiments. Although, cytotoxic responses were determined in vitro assays, 720 μg/kg EBR administration in SW480 tumor xenografts altered cell cycle-related proteins and exhibited a cytostatic effect. 720 μg/kg EBR significantly inhibited tumor progression and proved that as a steroid structured anti-cancer drug, it can be used as an adjuvant therapy with other known cytotoxic agents. EBR should further be evaluated as an anti-cancer agent with a higher dose administration on different tumor types.

Human participants and/or animals

This work involves mice and all the experiments were carried out at Acıbadem University, Transgenic Animals Laboratories, with the ethics committee approval (approval number: HDK-2019–34).

Informed consent

All authors are aware of the details of the research that are presented in the current manuscript and gave their consent to the publication.

Author contribution

As the grant holder, POY conceived and planned the experiments and contributed to interpreting the results. POY and KA wrote and organized the manuscript for publishing. As the project partners, AKK, EDA and ACG contributed to the interpretation of the results, and reviewed and edited the original draft.

CRediT authorship contribution statement

Pinar Obakan Yerlikaya: Conceptualization, Supervision, Methodology, Writing – original draft, Writing – review & editing. **Kaan Adacan:** Methodology, Software, Writing – original draft. **Ayse Karatug Kacar:** Methodology, Visualization, Investigation. **Ajda Coker Gurkan:** Visualization, Investigation. **Elif Damla Arisan:** Conceptualization, Methodology, Writing – review & editing.

Declaration of Competing Interest

No conflict of interest was declared by the authors.

Data availability

Data will be made available on request.

Acknowledgments

This work was funded by The Scientific and Technological Research Council of Turkey (TUBITAK; project number, 117Z727).

References

Adacan, K., Obakan Yerlikaya, P., 2020. Epibrassinolide activates AKT to trigger autophagy with polyamine metabolism in SW480 and DLD-1 colon cancer cell lines. Turk. J. Biol. Turk. Biyol. Derg. 44, 417–426. https://doi.org/10.3906/BIY-2005-37.

Adacan, K., Obakan-Yerlikaya, P., Arisan, E.D., Coker-Gurkan, A., Kaya, R.I., Palavan-Unsal, N., 2020. Epibrassinolide-induced autophagy occurs in an Atg5-independent manner due to endoplasmic stress induction in MEF cells. Amino Acids 52, 871–891. https://doi.org/10.1007/S00726-020-02857-W.

Almanza, A., Carlesso, A., Chintha, C., Creedican, S., Doultsinos, D., Leuzzi, B., Luís, A., McCarthy, N., Montibeller, L., More, S., Papaioannou, A., Püschel, F., Sassano, M.L.,

Skoko, J., Agostinis, P., de Belleroche, J., Eriksson, L.A., Fulda, S., Gorman, A.M., Healy, S., Kozlov, A., Muñoz-Pinedo, C., Rehm, M., Chevet, E., Samali, A., 2019. Endoplasmic reticulum stress signalling - from basic mechanisms to clinical applications. FEBS J. 286, 241–278. https://doi.org/10.1111/FEBS.14608.

Arakawa, S., Honda, S., Yamaguchi, H., Shimizu, S., 2017. Molecular mechanisms and physiological roles of Atg5/Atg7-independent alternative autophagy. Proc. Jpn. Acad. Ser. B Phys. Biol. Sci. 93, 378. https://doi.org/10.2183/PJAB.93.023.

Baek, N., Seo, O.W., Lee, J., Hulme, J., An, S.S.A., 2016. Real-time monitoring of cisplatin cytotoxicity on three-dimensional spheroid tumor cells. Drug Des. Devel. Ther. 10, 2155–2165. https://doi.org/10.2147/DDDT.S108004.

Belli, V., Sforza, V., Cardone, C., Martinelli, E., Barra, G., Matrone, N., Napolitano, S., Morgillo, F., Tuccillo, C., Federico, A., Dallio, M., Loguercio, C., Gravina, A.G., De Palma, R., Ciardiello, F., Troiani, T., 2017. Regorafenib in combination with silybin as a novel potential strategy for the treatment of metastatic colorectal cancer. Oncotarget 8, 68305–68316. https://doi.org/10.18632/ONCOTARGET.20054.

Bravo, R., Parra, V., Gatica, D., Rodriguez, A.E., Torrealba, N., Paredes, F., Wang, Z.V., Zorzano, A., Hill, J.A., Jaimovich, E., Quest, A.F.G., Lavandero, S., 2013. Endoplasmic reticulum and the unfolded protein response: dynamics and metabolic integration. Int. Rev. Cell Mol. Biol. 301, 215. https://doi.org/10.1016/B978-0-12-407704-1.00005-1.

Buchler, T., Pavlik, T., Melichar, B., Bortlicek, Z., Usiakova, Z., Dusek, L., Kiss, I., Kohoutek, M., Benesova, V., Vyzula, R., Abrahamova, J., Obermannova, R., 2014. Bevacizumab with 5-fluorouracil, leucovorin, and oxaliplatin versus bevacizumab with capecitabine and oxaliplatin for metastatic colorectal carcinoma: Results of a large registry-based cohort analysis. BMC Cancer 14, 1–7. https://doi.org/10.1186/1471-2407-14-323/TABLES/5.

Canavese, M., Santo, L., Raje, N., 2012. Cyclin dependent kinases in cancer potential for therapeutic intervention. Cancer Biol. Ther. 451, 451–457. https://doi.org/10.4161/cbt.19589.

Chen, Y., Zhang, W., Guo, X., Ren, J., Gao, A., 2019. The crosstalk between autophagy and apoptosis was mediated by phosphorylation of Bcl-2 and beclin1 in benzene-induced hematotoxicity. Cell Death Dis. 2019 (1010 10), 1–15. https://doi.org/10.1038/s41419-019-2004-4.

Coskun, D., Obakan, P., Arisan, E.D., Çoker-Gürkan, A., Palavan-Ünsal, N., 2015. Epibrassinolide alters PI3K/MAPK signaling axis via activating Foxo3a-induced mitochondria-mediated apoptosis in colon cancer cells. Exp. Cell Res. 338, 10–21. https://doi.org/10.1016/J.YEXCR.2015.08.015.

Dai, J.P., Zhao, X.F., Zeng, J., Wan, Q.Y., Yang, J.C., Li, W.Z., Chen, X.X., Wang, G.F., Li, K.S., 2013. Drug screening for autophagy inhibitors based on the dissociation of Beclin1-Bcl2 complex using BiFC technique and mechanism of eugenol on anti-influenza A virus activity. PLoS One 8. https://doi.org/10.1371/JOURNAL.PONE.0061026.

Ding, L., Cao, J., Lin, W., Chen, H., Xiong, X., Ao, H., Yu, M., Lin, J., Cui, Q., 2020. The roles of cyclin-dependent kinases in cell-cycle progression and therapeutic strategies in human breast cancer. Int. J. Mol. Sci. 21. https://doi.org/10.3390/IJMS21061960.

Edmondson, R., Broglie, J.J., Adcock, A.F., Yang, L., 2014. Three-dimensional cell culture systems and their applications in drug discovery and cell-based biosensors. Assay. Drug Dev. Technol. 12, 207–218. https://doi.org/10.1089/ADT.2014.573.

García-Reyes, B., Kretz, A.L., Ruff, J.P., Karstedt, S., von, Hillenbrand, A., Knippschild, U., Henne-Bruns, D., Lemke, J., 2018. The emerging role of cyclin-dependent kinases (CDKs) in pancreatic ductal adenocarcinoma. Int. J. Mol. Sci. 19. https://doi.org/10.3390/IJMS19103219.

Hardie, D.G., 2011. AMPK and autophagy get connected. EMBO J. 30, 634. https://doi.org/10.1038/EMBOJ.2011.12.

Hillary, R.F., Fitzgerald, U., 2018. A lifetime of stress: ATF6 in development and homeostasis. J. Biomed. Sci. 25, 1–10. https://doi.org/10.1186/S12929-018-0453-1/FIGURES/1.

Hsu, H.H., Chen, M.C., Day, C.H., Lin, Y.M., Li, S.Y., Tu, C.C., Padma, V.V., Shih, H.N., Kuo, W.W., Huang, C.Y., 2017. Thymoquinone suppresses migration of LoVo human colon cancer cells by reducing prostaglandin E2 induced COX-2 activation. World J. Gastroenterol. 23, 1171–1179. https://doi.org/10.3748/WJG.V23.I7.1171.

Hu, Q., Peng, J., Liu, W., He, X., Cui, L., Chen, X., Yang, M., Liu, H., Liu, S., Wang, H., 2014. Elevated cleaved caspase-3 is associated with shortened overall survival in several cancer types. Int. J. Clin. Exp. Pathol. 7, 5057.

Itakura, E., Mizushima, N., 2011. p62 Targeting to the autophagosome formation site requires self-oligomerization but not LC3 binding. J. Cell Biol. 192, 17–27. https://doi.org/10.1083/JCB.201009067.

Jeanes, A., Gottardi, C.J., Yap, A.S., 2008. Cadherins and cancer: how does cadherin dysfunction promote tumor progression? Oncogene 27, 6920–6929. https://doi.org/10.1038/ONC.2008.343.

Junjappa, R.P., Patil, P., Bhattarai, K.R., Kim, H.R., Chae, H.J., 2018. IRE1α Implications in endoplasmic reticulum stress-mediated development and pathogenesis of autoimmune diseases. Front. Immunol. 9, 1. https://doi.org/10.3389/FIMMU.2018.01289.

Kale, J., Osterlund, E.J., Andrews, D.W., 2017. BCL-2 family proteins: changing partners in the dance towards death. Cell Death Differ. 2018 251 25, 65–80. https://doi.org/10.1038/cdd.2017.186.

Kim, J., Kundu, M., Viollet, B., Guan, K.L., 2011. AMPK and mTOR regulate autophagy through direct phosphorylation of Ulk1. Nat. Cell Biol. 13, 132–141. https://doi.org/10.1038/NCB2152.

Kim, K.H., Lee, M.S., 2014. Autophagy–a key player in cellular and body metabolism. Nat. Rev. Endocrinol. 10, 322–337. https://doi.org/10.1038/NRENDO.2014.35.

Kohli, S.K., Bhardwaj, A., Bhardwaj, V., Sharma, A., Kalia, N., Landi, M., Bhardwaj, R., 2020. Therapeutic Potential of Brassinosteroids in Biomedical and Clinical Research. Biomol 2020 Vol. 10. https://doi.org/10.3390/BIOM10040572.

Li, W., Saud, S.M., Young, M.R., Chen, G., Hua, B., 2015. Targeting AMPK for cancer prevention and treatment. Oncotarget 6, 7365–7378. https://doi.org/10.18632/ONCOTARGET.3629.

Li, X., Zhou, Y., Li, Y., Yang, L., Ma, Y., Peng, X., Yang, S., Liu, J., Li, H., 2019. Autophagy: a novel mechanism of chemoresistance in cancers. Biomed. Pharmacother. 119, 109415 https://doi.org/10.1016/J.BIOPHA.2019.109415.

Li, Y., Cao, H., Jiao, Z., Pakala, S.B., Sirigiri, D.N.R., Li, W., Kumar, R., Mishra, L., 2010. Carcinoembryonic antigen interacts with TGF-{beta} receptor and inhibits TGF-{beta} signaling in colorectal cancers. Cancer Res 70, 8159–8168. https://doi.org/10.1158/0008-5472.CAN-10-1073.

Lin, L., Liu, A., Peng, Z., Lin, H.J., Li, P.K., Li, C., Lin, J., 2011. STAT3 is necessary for proliferation and survival in colon cancer-initiating cells. Cancer Res 71, 7226–7237. https://doi.org/10.1158/0008-5472.CAN-10-4660.

Linder, B., Kögel, D., 2019. Autophagy in cancer cell death. Biology 8. https://doi.org/10.3390/BIOLOGY8040082.

Lindqvist, L.M., Heinlein, M., Huang, D.C.S., Vaux, D.L., 2014. Prosurvival Bcl-2 family members affect autophagy only indirectly, by inhibiting Bax and Bak. Proc. Natl. Acad. Sci. U. S. A. 111, 8512–8517. https://doi.org/10.1073/PNAS.1406425111/SUPPL_FILE/PNAS.201406425SI.PDF.

Liu, T., Zhang, J., Chai, Z., Wang, G., Cui, N., Zhou, B., 2017. Ginkgo biloba extract EGb 761-induced upregulation of LincRNA-p21 inhibits colorectal cancer metastasis by associating with EZH2. Oncotarget 8, 91614–91627. https://doi.org/10.18632/ONCOTARGET.21345.

Liu, W.J., Ye, L., Huang, W.F., Guo, L.J., Xu, Z.G., Wu, H.L., Yang, C., Liu, H.F., 2016. p62 links the autophagy pathway and the ubiqutin-proteasome system upon ubiquitinated protein degradation. Cell. Mol. Biol. Lett. 21, 1–14. https://doi.org/10.1186/S11658-016-0031-Z/FIGURES/3.

Liu, Z., Lv, Y., Zhao, N., Guan, G., Wang, J., 2015. Protein kinase R-like ER kinase and its role in endoplasmic reticulum stress-decided cell fate. Cell Death Dis. 2015 (67 6) https://doi.org/10.1038/cddis.2015.183.

Marquez, R.T., Xu, L., 2012. Bcl-2:Beclin 1 complex: multiple, mechanisms regulating autophagy/apoptosis toggle switch. Am. J. Cancer Res 2, 214.

Martin, S.L., Kala, R., Tollefsbol, T.O., 2018. Mechanisms for the inhibition of colon cancer cells by sulforaphane through epigenetic modulation of microRNA-21 and Human telomerase reverse transcriptase (hTERT) down-regulation. Curr. Cancer Drug Targets 18, 97–106. https://doi.org/10.2174/1568009617666170206104032.

McCubrey, J.A., Lertpiriyapong, K., Steelman, L.S., Abrams, S.L., Yang, L.V., Murata, R. M., Rosalen, P.L., Scalisi, A., Neri, L.M., Cocco, L., Ratti, S., Martelli, A.M., Laidler, P., Dulinska-Litewka, J., Rakus, D., Gizak, A., Lombardi, P., Nicoletti, F., Candido, S., Libra, M., Montalto, G., Cervello, M., 2017. Effects of resveratrol, curcumin, berberine and other nutraceuticals on aging, cancer development, cancer stem cells and microRNAs. Aging (Albany NY) 9, 1477. https://doi.org/10.18632/AGING.101250.

Melling, N., Simon, R., Izbicki, J.R., Terracciano, L.M., Bokemeyer, C., Sauter, G., Marx, A.H., 2015. Expression of phospho-mTOR kinase is abundant in colorectal cancer and associated with left-sided tumor localization. Int. J. Clin. Exp. Pathol. 8, 7009.

Murray, S., Schell, K., McCarthy, D.O., Albertini, M.R., 1997. Tumor growth, weight loss and cytokines in SCID mice. Cancer Lett. 111, 111–115. https://doi.org/10.1016/S0304-3835(96)04519-3.

Ni, Y.L., Hsieh, C.H., Wang, J.P., Fang, K., 2018. Teroxirone motivates apoptotic death in tumorspheres of human lung cancer cells. Chem. Biol. Interact. 291, 137–143. https://doi.org/10.1016/J.CBI.2018.06.011.

Nishida, Y., Arakawa, S., Fujitani, K., Yamaguchi, H., Mizuta, T., Kanaseki, T., Komatsu, M., Otsu, K., Tsujimoto, Y., Shimizu, S., 2009. Discovery of Atg5/Atg7-independent alternative macroautophagy. Nature 2009. https://doi.org/10.1038/nature08455.

Obakan, P., Barrero, C., Coker-Gurkan, A., Arisan, E.D., Merali, S., Palavan-Unsal, N., 2015. SILAC-based mass spectrometry analysis reveals that epibrassinolide induces apoptosis via activating endoplasmic reticulum stress in prostate cancer cells. PLoS One 10. https://doi.org/10.1371/JOURNAL.PONE.0135788.

Obakan-Yerlikaya, P., Arisan, E.D., Coker-Gurkan, A., Adacan, K., Ozbey, U., Somuncu, B., Baran, D., Palavan-Unsal, N., 2017. Calreticulin is a fine tuning molecule in epibrassinolide-induced apoptosis through activating endoplasmic reticulum stress in colon cancer cells. Mol. Carcinog. 56, 1603–1619. https://doi.org/10.1002/MC.22616.

Ogata, M., Hino, S., Saito, A., Morikawa, K., Kondo, S., Kanemoto, S., Murakami, T., Taniguchi, M., Tanii, I., Yoshinaga, K., Shiosaka, S., Hammarback, J.A., Urano, F., Imaizumi, K., 2006. Autophagy is activated for cell survival after endoplasmic reticulum stress. Mol. Cell. Biol. 26, 9220. https://doi.org/10.1128/MCB.01453-06.

Peres, A.L.G.L., Soares, J.S., Tavares, R.G., Righetto, G., Zullo, M.A.T., Mandava, N.B., Menossi, M., 2019. Brassinosteroids, the sixth class of phytohormones: a molecular view from the discovery to hormonal interactions in plant development and stress adaptation. Int. J. Mol. Sci. 20. https://doi.org/10.3390/IJMS20020331.

Puissant, A., Robert, G., Fenouille, N., Luciano, F., Cassuto, J.P., Raynaud, S., Auberger, P., 2010. Resveratrol promotes autophagic cell death in chronic myelogenous leukemia cells via JNK-mediated p62/SQSTM1 expression and AMPK activation. Cancer Res 70, 1042–1052. https://doi.org/10.1158/0008-5472.CAN-09-3537.

Ray, A., James, M.K., Larochelle, S., Fisher, R.P., Blain, S.W., 2009. p27Kip1 inhibits cyclin D-cyclin-dependent kinase 4 by two independent modes. Mol. Cell. Biol. 29, 986–999. https://doi.org/10.1128/MCB.00898-08.

Riedl, A., Schlederer, M., Pudelko, K., Stadler, M., Walter, S., Unterleuthner, D., Unger, C., Kramer, N., Hengstschläger, M., Kenner, L., Pfeiffer, D., Krupitza, G., Dolznig, H., 2017. Comparison of cancer cells in 2D vs 3D culture reveals differences

in AKT-mTOR-S6K signaling and drug responses. J. Cell Sci. 130, 203–218. https://doi.org/10.1242/JCS.188102.
Samara, R.N., Laguinge, L.M., Jessup, J.M., 2007. Carcinoembryonic antigen inhibits anoikis in colorectal carcinoma cells by interfering with TRAIL-R2 (DR5) signaling. Cancer Res 67, 4774–4782. https://doi.org/10.1158/0008-5472.CAN-06-4315.
Shen, Y.H., Godlewski, J., Zhu, J., Sathyanarayana, P., Leaner, V., Birrer, M.J., Rana, A., Tzivion, G., 2003. Cross-talk between JNK/SAPK and ERK/MAPK pathways: sustained activation of JNK blocks ERK activation by mitogenic factors. J. Biol. Chem. 278, 26715–26721. https://doi.org/10.1074/JBC.M303264200.
Siegel, R.L., Miller, K.D., Fuchs, H.E., Jemal, A., 2021. Cancer statistics, 2021. Cancer J. Clin. 71, 7–33. https://doi.org/10.3322/CAAC.21654.
Siegel, R.L., Miller, K.D., Fuchs, H.E., Jemal, A., 2022. Cancer statistics, 2022. Cancer J. Clin. 72, 7–33. https://doi.org/10.3322/CAAC.21708.
Son, I.H., Chung, I.M., Lee, S.I., Yang, H.D., Moon, H.I., 2007. Pomiferin, histone deacetylase inhibitor isolated from the fruits of Maclura pomifera. Bioorg. Med. Chem. Lett. 17, 4753–4755. https://doi.org/10.1016/J.BMCL.2007.06.060.
Steigerová, J., Oklestkova, J., Levková, M., Rárová, L., Kolář, Z., Strnad, M., 2010. Brassinosteroids cause cell cycle arrest and apoptosis of human breast cancer cells. Chem. Biol. Interact. 188, 487–496. https://doi.org/10.1016/J.CBI.2010.09.006.
Steigerová, J., Rárová, L., Oklešťková, J., Křížová, K., Levková, M., Šváchová, M., Kolář, Z., Strnad, M., 2012. Mechanisms of natural brassinosteroid-induced apoptosis of prostate cancer cells. Food Chem. Toxicol. 50, 4068–4076. https://doi.org/10.1016/J.FCT.2012.08.031.
Suvorova, I.I., Pospelov, V.A., 2019. AMPK/Ulk1-dependent autophagy as a key mTOR regulator in the context of cell pluripotency. Cell Death Dis. 10. https://doi.org/10.1038/S41419-019-1501-9.
Tsai, S.C., Yang, J.S., Peng, S.F., Lu, C.C., Chiang, J.H., Chung, J.G., Lin, M.W., Lin, J.K., Amagaya, S., Chung, C.W.S., Tung, T.T., Huang, W.W., Tseng, M.T., 2012. Bufalin increases sensitivity to AKT/mTOR-induced autophagic cell death in SK-HEP-1 human hepatocellular carcinoma cells. Int. J. Oncol. 41, 1431–1442. https://doi.org/10.3892/IJO.2012.1579.
Wang, M., Kaufman, R.J., 2014. The impact of the endoplasmic reticulum protein-folding environment on cancer development. Nat. Rev. Cancer 14, 581–597. https://doi.org/10.1038/NRC3800.
Wesselborg, S., Stork, B., 2015. Autophagy signal transduction by ATG proteins: from hierarchies to networks. Cell. Mol. Life Sci. 72, 4721. https://doi.org/10.1007/S00018-015-2034-8.
Willows, R., Sanders, M.J., Xiao, B., Patel, B.R., Martin, S.R., Read, J., Wilson, J.R., Hubbard, J., Gamblin, S.J., Carling, D., 2017. Phosphorylation of AMPK by upstream kinases is required for activity in mammalian cells. Biochem. J. 474, 3059. https://doi.org/10.1042/BCJ20170458.
Wirawan, E., Vande Walle, L., Kersse, K., Cornelis, S., Claerhout, S., Vanoverberghe, I., Roelandt, R., De Rycke, R., Verspurten, J., Declercq, W., Agostinis, P., Vanden Berghe, T., Lippens, S., Vandenabeele, P., 2010. Caspase-mediated cleavage of Beclin-1 inactivates Beclin-1-induced autophagy and enhances apoptosis by promoting the release of proapoptotic factors from mitochondria. Cell Death Dis. 1, e18 https://doi.org/10.1038/CDDIS.2009.16.